SvedbergOpen
DISSEMINATION OF KNOWLEDGE
International Journal of Artificial Intelligence and Machine Learning
Publisher's Home Page: https://www.svedbergopen.com/
Research Paper Open Access

# Integration Learning Vector Quantization-Perceptron in the Mechanism Battery Charging Decision Model in AC-DC Hybrid Electrical Installations at Plant Factory

Iriansyah BM Sangadji[1] , Kudang Boro Seminar[2] , Sri Wahjuni, Heru Sukoco[3] , Iwa Garniwa MK[4]

[1]Department of Computer Science, Faculty of Mathematics and Natural Sciences, Bogor Agricultural University,Bogor, Indonesia Institut Teknologi PLN, Duri Kosambi, Cengkareng, West Jakarta Indonesia https://orcid.org/0000-0001-8665-6657, iriansyahsangadji@app.ipb.ac.id
[2]Department of Mechanical and Biosystem Engineering, Faculty of Agricultural Technology Bogor Agricultural University, Bogor, Indonesia https://orcid.org/0000-0001-8640-1646, kseminar@apps.ipb.ac.id
[3]Department of Computer Science, Faculty of Mathematics and Natural Sciences, Bogor Agricultural University,Bogor, Indonesiahttps://orcid.org/0000-0002-3929-1496, my_juni04@apps.ipb.ac.id https://orcid.org/0000-0002-1415-4022, hsrkom@apps.ipb.ac.id
[4]Department of Electrical Engineering, University of Indonesia, Depok, West Jawa, Indonesia https://orcid.org/ 0009-0004-2762-2122, iwa@ui.ac.id

**Abstract:** This study aims to optimize plant growth and development through the integration of learning vector quantization (LVQ) and a single-layer perceptron (SLP) for battery charging in the plant factory to optimize plant growth and development. During this analysis, the plant factory transmitted the concept of smart energy by adopting the relationship between the production and consumption of electrical energy of the Solar Power Plant (SPP) based on direct current (DC) and the service line (SL) following Alternating Current (AC). This combination was for charging the battery in the plant factory, and SPP had a limited time for electrical energy production due to the duration of sunlight. The scenario of sunlight duration and battery charge status ($SOC_{ES}$) in the three LVQ classifications, both SPP and battery, was input to the SLP for battery charging decisions. Charging scheduling was determined based on the time-duration relationship scenario between the SPP supply classification ($SPP_{Supl}$) and the state of charge ($SOC_{ES}$) of the battery. Perceptron decided the SOC on the battery and used the SPP and/or AC network. The results of models showed that the on-grid electrical energy supply process occurred when the state of consumption (0) was detected and applied to all battery clusters or $SPP_{Supl} > SOC_{MAX}$ values. In addition, the LVQ-SLP integration model produced accurate simulation results.

**Keywords:** LVQ, Perceptron, Battery, Charging, AC-DC Hybrid.

## 1. Introduction

The availability of electrical energy is absolutely needed in conducting the operational functions of the plant factory as a place for indoor production. Electrical energy originates from both the supply of service lines (SL), as well as electrical energy sources from new and renewable energy, with a special function for the supply needs of plant growth and development in the plant factory. The available sources are connected to the plant growth and development system through electrical installations that function

as a medium for the distribution of electrical energy. Moreover, the installation is finally connected to the plant growth and development container according to the respective growing phase.

This study will model the use of electrical installation architecture with AC-DC hybrid voltage for simultaneous operation in a plant factory. The integration (hybrid) is conducted by considering the use of the main electrical energy production, which uses new and renewable energy in a larger portion [1]. A method to optimize the use of several new and renewable energy sources integrated in the AC/DC grid can also be built [2].

The process discussed above shows electrical energy distributed used in the system has 2 (two) voltage characteristics, namely AC and DC, which are integrated, connected, and synergized between the two. The provision and use of electrical energy will be adjusted to the designation and character of the plant factory function, which is designed specifically for plant growth as well as development. This system includes several coordinated relationships between Solar Power Plant (SPP) -battery, consumer SL-battery, and the supply of electrical energy consumption load. In managing these relationships, it is necessary to determine the feasibility and definition of the regulation governing the use of electrical energy sources. These regulations should be associated with the appropriate electrical installation standards to ensure effective distribution of electrical energy to meet consumption demands.

Electrical energy supply network installations that are built by accommodating AC-DC hybrid voltage regulation are designed to facilitate the integration of new and renewable energy, as most operate on DC voltage. The integrated arrangement of multiple AC and DC converters enables efficient incorporation of these renewable energy sources, connecting to the grid and distributing electrical energy to various loads. In addition, the system is supported by a battery storage unit, ensuring the smart grid hybrid concept may be the solution to future utility needs [3].

There is a scenario that the supply of electrical energy can be provided directly by SPP (on the grid) [4]. However, the supply of electrical energy in this way cannot be optimal due to the condition that the sun is intermittent [5]. Energy management should be implemented to regulate the storage of electrical energy from the SPP to the battery to address the limitation. This allows the stored energy to be used and function properly in an off-grid mode when sunlight is reduced or at night. The energy management system on the battery will determine when to charge or discharge.

The use of the multi-layer perceptron (MLP) method in studies on energy management systems in batteries has been widely conducted [7]. However, the use of the perceptron method with a single layer is still not widely found in studies. The single-layer perceptron (SLP) method is more efficient in implementing the integration of neural network-based embedded systems for energy storage management. Given this gap, the energy storage management needs to be addressed, and the present study will use a perceptron method, which is a computational model in artificial neural networks. The perceptron in this study functions for handling charging as well as discharging to store or distribute electrical energy produced by Photovoltaic (PV) to the load and battery.

## 2. Comprehensive Theoretical

Optimization of energy availability and consumption with an AC-DC hybrid voltage synergy should be quantifiable and show reliable function. The management of the performance function will be conducted through a theoretical computing model method with interconnected sources of electrical energy, including SPP, Battery, and SL.

### 2.1. Plant Factory

The conditioning of the plant growth and development environment in the plant factory requires careful consideration of both the factors of energy readiness and the efficiency of electrical energy consumption. The need for electrical energy consumption is related to being able to produce good food crop products by optimizing artificial light irradiation, such as the use of LED lights, irrigation regulation, temperature, and humidity of the growing environment of plants, and the treatment of nutrition. These processes can be implemented with efficient electrical energy in DC voltage. The source of electrical energy needed by the plant factory will be managed and regulated to ensure that the supply of energy can be more efficient as well as effective to support the functional needs of the plant factory. Eventually, optimal plant growth and consumption efficiency of electrical energy operations can be achieved simultaneously. Electrical energy consumption in plant factories that contribute approximately 30% of the total operating costs includes artificial light, air conditioning, and pumps. The development and study of plant factory energy

management systems that operate in a semi-automated way in regulating electrical energy consumption to support plant growth and development have not fully used the machine learning model [8]. However, a machine learning model is needed in the implementation of smart plant factories, especially the regulation of smart electrical energy consumption efficiency [9]. These factors can be developed by considering the anticipation and mitigation of negative impacts on the supporting environment for plant growth and development through a machine learning-based warning system [10].

### 2.1.1. Hybrid AC-DC electrical energy installation

The installation of direct current (DC) electrical distribution networks powered by renewable energy in buildings is currently increasing due to the use of energy distribution and storage systems, such as batteries [11]. Although the power grid available in Indonesia currently still uses alternating current (AC) distribution, the DC in this study will be integrated into the system as a hybrid electrical installation network.

Hybrid AC/DC electrical installations are designed to use different types of renewable energy sources and can meet the requirements of different types of loads. Following the discussion, hybrid microgrids consist of DC sub-grids, AC sub-grids, and interface sub-grids of both [12]. Studies on hybrid installations used in buildings have been conducted for the functional needs of commercial areas [13], small buildings [14], and others. In this study, the plant factory installation is aimed at the use of electrical energy supply for plant growth and development, as shown in Figure 1.

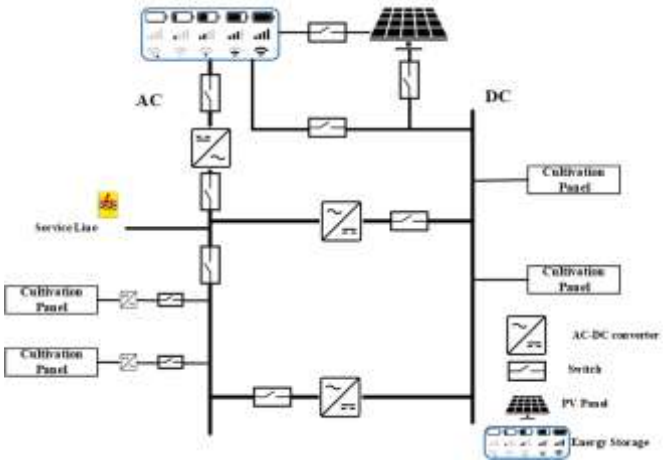


**Fig.1. Plant factory hybrid AC-DC electrical installation**

The topology of the AC-DC hybrid installation, as shown in Figure 1, shows that there are an AC Bus and a DC Bus connected to the respective loads. The load on an AC or DC Bus can be flexibly increased or decreased by considering the provision of the installed electrical energy load. There are three sources of energy, namely, energy sources from SL, batteries, and direct SPP. In this study, energy management from the three energy sources should be handled to use the perceptron method to ensure that the availability of electrical energy can meet the consumption of the load side optimally.

### 2.1.2. Hybrid AC-DC scenarios

The use of AC and DC hybrids follows the scenario relationship as shown in Figure 2.

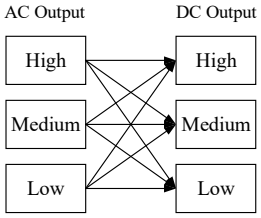


**Fig.2. AC-DC relationship**

Hybrid AC/DC system model for maximum electrical energy supply in installations Fig 1 and Fig 2 signifies following the appropriate settings for the formulation:

$$E_{Max} = E_{AC} + E_{DC} \quad (1)$$

Where $E_{Max}$ Total is the Total Supply of Electrical Energy from AC Power ($E_{AC}$) and DC Power ($E_{DC}$). The $E_{Max}$ value in this study is the accumulation of the amount originating from AC electrical energy sources, namely subscription SL and DC sources that include SPP as well as batteries. The value of AC electrical energy has been determined by the value limit based on government policy. Meanwhile, the limit of DC energy value depends on the number of panels integrated in a SPP and the amount of available battery capacity. DC electrical energy generated by SPP cannot be fully used due to features including environmental factors, geography [15], equipment efficiency [16], and seasons or weather. Regarding equipment efficiency, the electrical energy that can be absorbed by batteries ranges from 70%-85%, or only [17].

## 2.2. Solar power plant (SPP)

A major source of electrical energy from new and renewable energy is the solar power plant (SPP). This system generates electricity produced by converting sunlight into electrical energy. Sunlight containing photons through certain mechanisms on solar panels [18] is converted into electrical signals that are often referred to as Photovoltaic (PV). The output of PV panels is entirely dependent on the climate [19]. Energy production is typically higher when there is abundant sunlight in the dry season and significantly lower during rainy conditions. Due to this variability, forecasting based on accurate measurements of electrical energy production patterns from SPP is essential, considering economic reasons due to the uncertainty factor in different seasons and changes in meteorological conditions. The data from the measurement results in this study is on a SPP with a capacity of 38 kwp as shown in Figure 3.

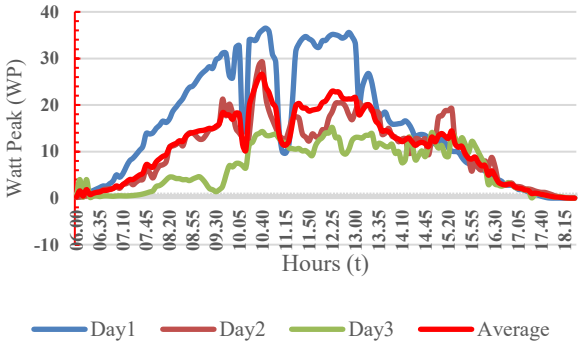


**Fig.3. Pattern of solar energy measurement**

The pattern of the measurement results of electrical energy produced by the SPP in Figure 3 shows that the best time for high electrical power production from solar panels is around 10.00 AM to 02.30 PM. The electrical energy produced by a SPP is calculated according to equation (2)

$$P = I.V \quad (2)$$

Where,
P = Watt-Hours
I=Amprere-Hours
V=Volt

Figure 3 shows the amount of watt-peak (WP) electrical energy produced by the PV power plant. The high or low WP at a certain unit of time depends on the number of solar panels ($Panel_i$) in a topology [20] to optimally "absorb" the existing solar energy to be converted into electrical energy. Each solar panel ($Panel_i$) is formed by having a different amount of absorption capacity and producing electrical energy

depending on the surface area set by the manufacturer. In this study, the optimal scenario of using 60% of the electrical energy produced by the SPP will be used for the supply of plant factory energy. The optimal energy use model shows that the maximum energy produced by a SPP is the total accumulated electrical energy produced by all its connected solar panels, according to equation (3).

$$E_{SPP} = T \sum_{i=1,2...n}^{N} Panel_i \quad (3)$$

Where,
$E_{SPP}$ = Solar power plant energies
$Panel_i$=Solar power plant panels.

The value of 38 kWp comes from $E_{SPP}$ based on the accumulation of electrical energy generated from various solar panels integrated at the place where this study is conducted.

When the use of $E_{SPP}$ is 60%, the optimal electrical energy of the SPP can be modeled according to equation (4).

$$EOP_{SPP} = E_{SPP} - (40\%. E_{SPP}) \quad (4)$$

$EOP_{SPP}$ = Optimal energy at $E_{SPP}$

This signifies that the value based on equation (4) of the process, $EOP_{SPP}$ in this study, is known from 38 kWp to 22,200 Wp or 22.2 kWp.

## 2.3. Battery (Energi Storage)

The use of batteries or energy storage can have a dual function, namely as a source of electrical energy with the amount of capacity to be distributed into the installation network. In addition, the batteries can also be charged for the storage of electrical energy reserves.

The electrical energy capacity that can be accommodated or distributed is often stand-alone or interconnected, forming a matrix according to the amount of energy storage and forming clusters of energy sources. In determining the amount of battery capacity to be used, it should be adjusted to the nominal voltage standard of the battery product that has been set. The calculation of the battery capacity to be used follows equation (5).

$$EB = Ah. V \quad (5)$$

Where,
EB= Battery energies
Ah = Battery Capacity
V = 12 VDC

## 2.4. Solar power plant – Battery model relation

There is a functional relationship between energy storage (Battery) and SPP. This relationship operates in two primary modes. First, the electrical energy generated by solar panels can be directly supplied to the load on the grid. Second, the energy produced by solar panels can be stored in the battery and later distributed to the plant factory when needed in an off-grid mode**.**

Solar panels start generating electrical energy when the sun starts to rise until the sunlight disappears at sunset. The pattern of electrical energy produced during this time span is obtained from the measurement of the recording device on the SPP during that period.

In the relationship model between SPP and Battery, the electrical energy storage system can be integrated by defining different power conversion system layouts for the Charging and Discharging strategy model. Considering a layout that joins to the AC connection, the Battery is connected to the AC side of the system through an additional inverter. On the other hand, the Battery is connected to the DC side, with or without a dedicated DC-DC converter, and no additional inverter is required in the DC clutch layout [21]. In this study, the pattern of electrical energy produced by SPP can be classified by dividing into three categories with a qualitative scheme, namely, High, Medium, and Low.

$$SPP_{Supl}, \begin{cases} High, SPP_{Supl} \geq 66\% \\ Medium, 30\% \leq SPP_{Supl} < 66\% \\ Low, SPP_{Supl} < 30\% \end{cases} \quad (6)$$

Where,
$SPP_{Supl}$ = Solar power plant supplies energy

The Charging relationship model, when it uses the electrical energy supplied by the SPP, should be matched and mapped with the condition of $SPP_{Supl}$ against $SOC_{ES}$. The matching model between the two is shown in Figure. 7.

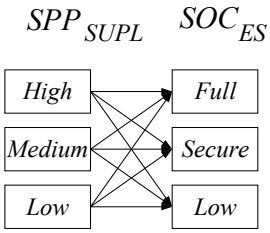


**Fig.4. SPP – Batteries Charging**

Figure 4 shows the relationship of each SPP energy supply status as classification (6) to the battery as classification (8).

## 2.5. Charging period

The management of charging scheduling and the length of battery charging time depends on the topology of the interconnectedness of the battery matrix being built, and the amount of electricity that should be supplied by the SPP, SL, or subscription. The state of the von the State of Charge (SOC) value, or available energy in the battery. Based on the literature, the minimum SOC value is < 30% of the energy still stored in the battery, and the maximum SOC value is 95%. The SOC value for the safety of the availability of electrical energy in the battery is 30%. Moreover, Depth of Discharge (DOD) can be interpreted as the energy use (consumption) value of the battery, which can be obtained with a minimum SOC value of 30%.

When $DOD_{Max} = SOC_{Min}$, the process of charging and discharging electrical energy can be conducted. DOC is the status of the level of electrical energy that has been used in a battery. During this process, the system decides to charge or discharge by observing the feasibility of the energy status available from the SPP or SL. The state of the energy condition, SOC, is shown in Figure 5.

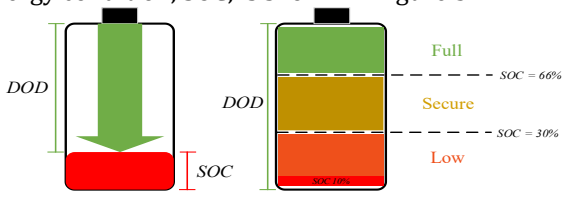


**Fig.5. Battery Status**

Energy for Charging can come from SPP and from the electrical energy SL network. Two ways of charging are conducted, namely, normal and fast, where normal charging follows equation (7):

$$Time_{Charging}(Hours) = \frac{EB_i}{EOP_{SPP/12V}} \quad (7)$$

Where,

EB= Battery energies
$EOP_{SPP}$ = Optimal energy at $E_{SPP}$

From equation (7), the difference between the charging methods is the AH Capacity sent to the Energy Storage from the SPP Panel. A higher AH Capacity leads to faster charging time, signifying that fast charging can be achieved by increasing the AH value from SPP to Battery. The charging flowchart process in accordance with the relationship between the SPP and the battery is shown in Figure 6.

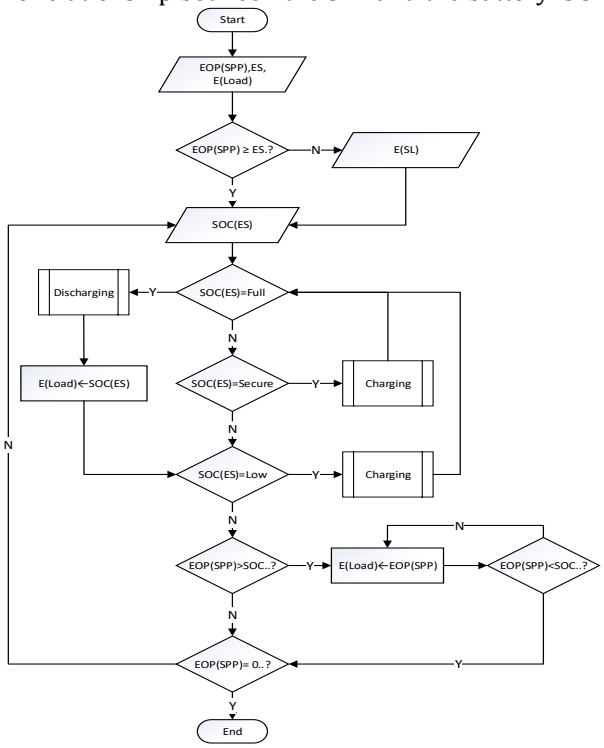


**Fig. 6. Charging Management**

Figure 6 shows the charging, on-grid, and off-grid mechanisms of SPP with battery usage. There are dynamic conditions for the energy supply of the SPP, and the energy load for charging is adjusted to the available electrical energy capacity of the battery. During the process, classification decisions using machine learning can be achieved depending on the condition of the quantity, supply energy, and energy contained in the battery (SOC).

## 2.6. Battery Topology

Batteries function as suppliers and stores of electrical energy, and can be arranged in the form of a matrix topology to improve the reliability of the electrical energy supply. A major element in any energy storage system is the ability to monitor, control, and optimize the reliability of its performance singly or incorporated into multiple batteries in an energy storage system. This management scheme is known as the battery management system, which is an important unit in the operation of the electrical energy grid. The process is performed to improve the reliability of battery performance in a system.

The battery topology can be arranged into one or several connected battery pools according to the required electrical energy storage. The topology used in this study is divided into four clusters, and the method requires defining the power of each cluster based on the number of batteries in an integrated collection. According to classification (18), Clusters 1 and 2 each have a power capacity of 4x1800 W, Cluster 3 has a size of 8x1800 W, and Cluster 4 has a capacity of 16x1800 W, respectively. This signifies that the qualitative classification of the energy of each battery cluster is as follows.

$$SOC_{ES}, \begin{cases} \text{Full }, 66\% \leq SOC \leq SOC_{Max} \\ \text{Secure}, 30\% \leq SOC < 66\% \\ \text{Low}, SOC_{MIn} \leq SOC < 30\% \end{cases} \quad (8)$$

Where,
$SOC_{ES}$ = Battery capacity
$SOC_{Max}$ = Maximal Battery Capacity
$SOC_{Min}$ = Minimal Battery Capacity

Similar to equation (3), compiling an energy cluster from a set of several energy storage (batteries) is as follows:

$$ES_i = \Delta t \sum_{i=1,2,\ldots,n}^{n} EB_i \quad (9)$$

Where,
$ES_i$: Energi Storage at i
$EB_{1\text{-}n}$: A set of connected batteries to increase the storage capacity and supply of electrical energy, where the $ES_i$ value depends on the total capacity of the integrated battery cluster.

## 2.7. Learning Vector Quantization (LVQ)

LVQ1 is the first variant of the LVQ network, and the following algorithm shows its training process. Basically, for every input vector, the winner prototype vector is identified. When the class label of the input vector equals the class of the winner prototype, it is adjusted to move closer to the input vector, ensuring that the vector will be correctly classified in subsequent iterations.

Step 1 Initialization of prototype vectors, namely, weights: $Y_j = (w_{1j}, w_{2j} \ldots w_{nj})$
Step 2 Decide the number of prototype vectors for each class.
Step 3 Determine the learning rate $\delta \in (0,1)$, and the number of maximum epochs.
Step 4 For each x vector in the training set
Step 5 For each prototype vector w
Step 6 Calculate the distances between input vectors and prototype vectors with Euclidean distance as shown in Equation 10.

$$d(x, w) = \sum_{i=1}^{n} \sum_{j=1}^{m} (x_i - w_{ij})^2 \quad (10)$$

where $n$ is the number of input vectors in the training set, and $m$ is the number of prototype vectors.
End
Step 7 Find the winner prototype vector w.
Step 8 Update the winner prototype vector indicated in Equations 11 and 12.

$$w_{new} = w_{old} + \delta(x - w_{old}), \text{if } P = C \quad (11)$$
$$w_{new} = w_{old} - \delta(x - w_{old}), \text{if } P \neq C \quad (12)$$

where $C$ is the class of the input vector, and $P$ is the class of the winner prototype vector.
End
Step 9 Decrease the learning rate, $\delta$, with a decreasing rate, $\beta \in (0,1)$, as shown in step 4.

## 2.8. Perceptron

A perceptron is a simple algorithm compared to other machine learning models. The method uses a system or model that wants the output to be only two states or boolens. The process of determining charging and discharging is only an example of these two conditions. Perceptron is the proposed algorithm to be used in the completion of this study. The output of the algorithm is two states, namely 0 and 1, commonly called binary, or -1 and 1 (bipolar). The perceptron algorithm and architecture [22] during the analysis are as follows:

Algorithm Perceptron Pseudo-code

**Input**:

Vector x Label 0 = Negative (N) input
Label 1 = Positive (P) input
**Training**:
Randomly initialize w misclassification != 0 x ∈ N and $\sum_{i=0}^{n} w_i \; x \; x_i \geq 0$ w = w − x
x ∈ P and $\sum_{i=0}^{n} w_i \; x \; x_i \geq 0$ w = w + x n i=0 wi × xi < 0 w = w + x
**Output**:
Parameters w

The perceptron model architecture uses a simple perceptron, commonly called a SLP, as shown in Figure 7.

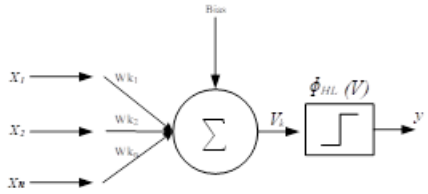


**Fig. 7. SLP Architecture**

The perceptron model is a machine learning architecture characterized by a learning process to determine the optimal weights in the network. The weighting is conducted to enable an effective classification function of the input data. Two processes should occur before the perceptron architecture can be implemented. This includes the learning process to achieve the optimal weight of the architecture and the simulation process to ensure the output of the model. Several studies have used MLP models to achieve improved predictive performance [23].

## 3. Methodology

The modeling of the electrical energy pattern produced by the SPP, as well as the battery charging scheduling mechanism based on these patterns, was evaluated through simulation and model testing. This process was conducted according to the methodology as shown in Figure 8.

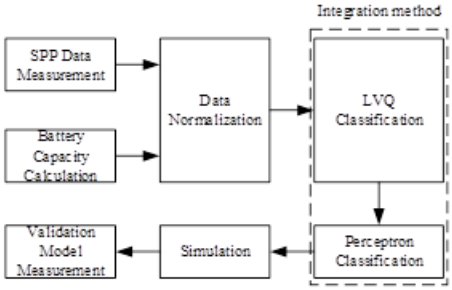


**Fig.8. Methodology**

### 3.1. SPP Capabilities and Status

Based on classification (6), the status of the electrical energy supply of the SPP was as follows:

$$SPP_{Supl}, \begin{cases} \text{High}, SPP_{Supl} \geq 1387 \\ \text{Medium}, 937 \leq SPP_{Supl} < 1387 \\ \text{Low}, SPP_{Supl} < 937 \end{cases}$$

In battery charging, an adequate Ampere-Hour (AH) value was needed according to the amount of battery capacity to be charged. The conversion was performed by determining the value of ampere (I)

from equation (2) to $I = \frac{P}{V}$. This allowed the electrical energy requirement from the SPP for battery charging to be calculated. The amount of value (I) depended on the result obtained from Equation (3). As the $E_{SPP}$ increased, a greater number of battery capacities could be charged simultaneously.

Values greater than 1388 represented the lower limit of the 66% high qualitative value limit. The range of 937–1387 was the limit of the medium qualitative value class, while the value of 936 was the low qualitative high limit (33%).

## 3.2. Battery Capabilities and Status

The calculation of battery storage capacity was conducted based on equations (7) and (8) according to the battery topology as shown in Figure 6. The topology was divided into four clusters, and it was necessary to define the status of each cluster. Based on classification (18) for Clusters 1 and 2, each had a power capacity requirement of 4x1800, with the arrangement as follows.

$$SOC_{1,2}, \begin{cases} \text{Full}, 4728 < SOC \leq 7164 \\ \text{Secure}, 2149 \leq SOC \leq 4728 \\ \text{Low}, SOC < 2149 \end{cases}$$

Cluster 3 with a size of 8x1800 was:

$$SOC_3, \begin{cases} \text{Full}, 9029 < SOC \leq 13680 \\ \text{Secure}, 4104 \leq SOC \leq 9029 \\ \text{Low}, SOC < 4104 \end{cases}$$

Cluster 4 with a size of 16x1800 was:

$$SOC_4, \begin{cases} \text{Full}, 18058 < SOC \leq 27360 \\ \text{Secure}, 8208 \leq SOC \leq 18058 \\ \text{Low}, SOC < 8208 \end{cases}$$

The process showed that the total of all clusters with a full lower limit was $\sum_{i=1,\dots,4} SOC_i, (\text{Full}) \geq 36.583$ WP. In addition, the lower upper limit was $\sum_{i=1,2,3,4} SOC_i, (\text{Low}) \leq 16.610$ WP.

The results of the counter adjusted to the capacity of electrical energy in the battery (SOC) were shown in Table 1. The calculation of charging time according to the reference used equation (7):

**Table 1. Battery capacity calculation**

| Battery (Qty) | SOC (hours) | | | | | |
|---|---|---|---|---|---|---|
| | 30 | 50 | 66 | 70 | 80 | 90 |
| 1 | 0,06 | 0,04 | 0,03 | 0,02 | 0,02 | 0,01 |
| 2 | 0,14 | 0,12 | 0,11 | 0,11 | 0,10 | 0,09 |
| 4 | 0,30 | 0,28 | 0,27 | 0,27 | 0,26 | 0,25 |
| 8 | 0,62 | 0,61 | 0,60 | 0,59 | 0,58 | 0,58 |
| 16 | 1,27 | 1,26 | 1,24 | 1,24 | 1,23 | 1,22 |

SOC was the energy state in a battery with the smallest value of 30% to 90% charge. Battery quantity describes the number of batteries integrated in a cluster. All values were calculated using Equation (7) for charging duration and Equation (9) for the battery capacity in the cluster. As shown in Table 1, the total quantity of four batteries (clusters 1 & 2) had a duration ranging from 0.30 (30%) to 0.25 hours (90%). For eight batteries (cluster 3), the duration ranged from 0.62 (30%) to 0.58 hours (90%). Finally, for sixteen batteries (cluster 4), the duration ranged from 1.27 (30%) to 1.22 hours (90%).

## 3.3. SPP-Battery charging mapping scenarios.

The relationship that occurred between the charging calculation time based on the battery capacity in Table 1, the calculation of classification (6) on SPP, and classification (8) on batteries (SOC) defined the overall system behavior. This value mapping led to a charging scenario as shown in Table 2.

**Table 2: SPP to battery charging duration**

| $SPP_{Supl}$ | $SOC_{ES}$ | $SPP_{Status}$ | Duration (Hour) | | | |
|---|---|---|---|---|---|---|
| | | | $SOC_1$ | $SOC_2$ | $SOC_3$ | $SOC_4$ |
| High | Full | On G *) | DSC | DSC | DSC | DSC |
| | Secure G | On G \| Off | 0,28 – 0,41 | 0,28 – 0,41 | 0,60 – 0,84 | 1,25 – 1,70 |
| | Low G | On G \| Off | 0,31 – 0,41 | 0,31 – 0,41 | 0,63 – 0,84 | 1,28 – 1,71 |
| Medium | Full G | On G \| Off | 0,25 – 0,53 | 0,25 – 0,53 | 0,60 – 1,18 | 1,24 – 2,46 |
| | Secure G | On G \| Off | 0,28 – 0,59 | 0,28 – 0,59 | 0,60 – 1,23 | 1,25 – 1,70 |
| | Low G | On G \| Off | 0,31 – 0,41 | 0,31 – 0,41 | 0,63 – 0,84 | 1,28 – 1,71 |
| Low | Full G | On G \| Off | 0,49 – 0,53 | 0,49 – 0,53 | 1,13 – 1,18 | 2,41 – 2,46 |
| | Secure G | On G \| Off | 0,54 – 0,59 | 0,54 – 0,59 | 1,18 – 1,23 | 2,47 – 2,51 |
| | Low | Off G **) | > 0,61 | > 0,61 | >1,25 | > 2,53 |

*) = On Grid
**)= Off Grid

Table 2 showed the relationship (Figure 4) between SPP and battery capacity (SOC) that led to the duration of the required charging time. In the condition of the High → Full relationship, all electrical energy produced by the SPP could be directly distributed to the plant factory load, while battery energy was not used. In the condition of the Low → Low relationship, the condition was full charging, and the SPP could not directly distribute its electrical energy.

## 3.4. Data Normalization

The distribution of battery cluster charging states was arranged using the SLP neural network model method. In the input, the process, and the result value using the perceptron method were in the form of normalized vector values. The existing data, including SPP and battery data, should be normalized using equation (10):

$$N_{Norm} = \frac{N - N_{Min}}{N_{Max} - N_{Min}} (10)$$

Where,
$N_{Norm}$ = Normalization Value
$N_{Min}$ = Minimal Value
$N_{Max}$= Maximal Value

The duration charging scenarios in Table 2 showed the scenarios to be implemented and the parts of the perceptron method feature extraction. The relationship between the value of SPP and batteries, in addition to being a classifier in determining charging as well as discharging, also determined the action of providing electrical energy to be supplied off the grid or on grid.

## 3.5. Perceptron Classification

Training was needed to determine the final optimization weight of the SLP, as shown in Figure 8, to ensure that the perceptron method was implemented for charging and discharging scenarios. The data training process was conducted following a pseudo-code perceptron algorithm.

The training process of the perceptron method used the MATLAB application by preparing training data, which consisted of input ($SPP_{Supl}$ & $SOC_{ES}$) as well as target data ($SOC_{1,2,...,4}$), as shown in Table 3 and architecture in Figure 7.

**Table 3. Perceptron charging mapping**

| $SPP_{Supl}$ | $SOC_{ES}$ | Battery Charging | | | |
|---|---|---|---|---|---|
| | | $SOC_1$ | $SOC_2$ | $SOC_3$ | $SOC_4$ |
| 1 | 1 | 0 | 0 | 0 | 0 |
| | 0,5 | 0 | 0 | 0 | 0 |
| | 0 | 1 | 1 | 1 | 1 |
| 0,5 | 1 | 0 | 0 | 0 | 0 |
| | 0,5 | 0 | 0 | 0 | 0 |
| | 0 | 1 | 1 | 1 | 1 |
| 0 | 1 | 0 | 0 | 0 | 0 |
| | 0,5 | 1 | 1 | 0 | 1 |
| | 0 | 1 | 1 | 1 | 1 |

$SPP_{Supl}$ represented the status of the electrical energy supply from SPP, and $SOC_{ES}$ was to explain the energy status of each battery cluster that was prepared. The $SOC_{1,2,...,4}$ status, with a value of 1 explained the charging position, and the value of 0 was non-charging. In addition, SL charging (charging with AC) was determined in scenarios related to SPP-SOC 0,5-0 and 0-0.

### 3.6. Model validation

The status of both SPP and batteries (SOC) was defined or normalized into numbers (0), (0.5), and (1) according to equation (10). These values were determined as class limits for three categories in modeling electrical energy supply systems based on classifications (6) and (8). Since the process was the definition of class boundaries, a class had more than one value in it. During the analysis, the simulation was conducted with a combination of the actual measurement event values that reflected the class limit state performed on the SPP on one day at 10.00 AM–15.00 PM, and also with the class value limit on the battery. The test results with the optimal final weight in Figure 11 followed the target value as shown in Table 4.

**Table 4. LVQ-Perceptron Integration validation model**

| | $SPP_{Supl}$ (WP) | $SOC_{ES}$ (W) | LVQ Result | Battery Charging | | | | Perceptron Result |
|---|---|---|---|---|---|---|---|---|
| | | | | $SOC_1$ | $SOC_2$ | $SOC_3$ | $SOC_4$ | |
| 1. | 16644 – 38000 (1) | 7164 – 28800 (1) | √ | 0 | 0 | 0 | 0 | √ |
| 2. | | 2149 – 8207,9 (0.5) | √ | 0 | 0 | 0 | 0 | √ |
| 3. | | 2148,9 – 8202 (0) | √ | 1 | 1 | 1 | 1 | √ |
| 4. | 11244 – 16643 (0.5) | 7164 – 28800 (1) | √ | 0 | 0 | 0 | 0 | √ |
| 5. | | 2149 – 8207,9 (0.5) | √ | 0 | 0 | 0 | 0 | √ |
| 6. | | 2148,9 – 8202 (0) | √ | 1 | 1 | 1 | 1 | √ |
| 7. | < 11244 (0) | 7164 – 28800 (1) | √ | 0 | 0 | 0 | 0 | √ |
| 8. | | 2149 – 8207,9 (0.5) | √ | 1 | 1 | 0 | 1 | √ |
| 9. | | 2148,9 – 8202 (0) | √ | 1 | 1 | 1 | 1 | √ |

## 4. Result and discussion

### 4.1. Duration of charging scheduling

Based on the relationship between Table 3 (charging scenario) and 4 (simulation results), a decision was made regarding the scheduling of charging and its duration, as shown in Table 5.

**Table 5. Scheduling Charging Based on Integrated LVQ-Perceptron**

| $SPP_{Supl}$ (WP) | $SOC_{ES}$ (W) | Battery Charging (Hours) | | | | Relation $SPP_{Supl}$ - $SOC_{ES}$ | | |
|---|---|---|---|---|---|---|---|---|
| | | $SOC_1$ | $SOC_2$ | $SOC_3$ | $SOC_4$ | $SOC_{1,2}$ | $SOC_3$ | $SOC_4$ |
| 14918,4 | 1440 | 0,31 – 0,41 | 0,31 – 0,41 | 0,63 – 0,84 | 1,28 – 1,71 | MED - LOW | MED - LOW | MED – LOW |
| 8347,2 | 4723,2 | 0,54 – 0,59 | 0,54 – 0,59 | 0 | 1,28 – 1,71 | LOW – SEC | - | MED – LOW |
| 7281,6 | 4492,8 | 0,54 – 0,59 | 0,54 – 0,59 | 0 | 1,28 – 1,71 | LOW – SEC | - | MED – LOW |
| 7992 | 5068,8 | 0,49 – 0,53 | 0,49 – 0,53 | 0 | 1,28 – 1,71 | LOW – FUL | - | MED – LOW |
| 12432 | 5241,6 | 0 | 0 | 0 | 0 | - | - | - |
| 22200 | 1440 | 0,31 – 0,41 | 0,31 – 0,41 | 0,63 – 0,84 | 1,28 – 1,71 | HI – LOW | HI - LOW | HI – LOW |
| 9235,2 | 10828,8 | 0,49 – 0,53 | 0,49 – 0,53 | 0 | 0 | LOW – FUL | - | - |
| 8524,8 | 9792 | 0,25 – 0,53 | 0,25 – 0,53 | 0 | 1,25 – 1,70 | MED – FUL | - | MED - SEC |
| 12964,8 | 11980,8 | 0,49 – 0,53 | 0,49 – 0,53 | 0 | 0 | LOW - FUL | - | - |

Table 5 shows the scheduling by the perceptron model along with the charging duration required for the battery from the electricity produced by the SPP. The relationship between $SPP_{Supl}$ and $SOC_{ES}$ presented the production of electrical energy by dynamic SPP and the ability to store energy from batteries. The duration of the time (hours) needed for the charging process depended on the energy value (SOC) that was still in each battery cluster. The value of 0 in this study was interpreted as a discharging process. Based on the relationship between the value of energy produced by the SPP and the capacity of each battery cluster, the $SOC_{1,2}$ cluster had a relationship between the value of low electrical energy storage capacity, MEDIUM–LOW and HIGH–LOW, with a charging time of 0.31–0.41 hours. The relationship between the value of medium electrical energy storage capacity (Secure), LOW–SECURE, required a charging time of 0.54–0.59 hours. In addition, the relationship between the value of full electrical energy storage capacity (Full) LOW/MEDIUM/FULL–FULL required a charging time of 0.25–0.59 hours.

## 5. Conclusion

In conclusion, the method using the integrated LVQ-SLP model required defining the values based on feature extraction from the SPP measurement data. The relationship between solar power generation and the SOC of the battery during the optimal period (10.00 AM – 15.00 PM) determined the precision of the charging or discharging schedule and its duration.

The use of the perceptron model in hybrid electric installations (AC-DC) in plant factories supported the implementation of battery charging scheduling based on electrical energy generated by the SPP. This method served as a basis for the development of automation processes for learning systems by adding SL (AC). The characteristic of a plant factory is the use of electrical energy for the growth and development of plants in a closed room. Each type of plant has different features of its growth and development phases, signifying that the electrical energy required for each phase is also different. The LVQ-SLP model method, with the methodology discussed, can be used for this purpose.

## Author Contributions

I.B.M.: conceptualization, investigation, writing an original draft; K.B.S.: methodology, reviewing and editing; S.W.: research design, data analysis, investigation, model investigating; H.S.: conceptualization, data curation; I.G.M.: conceptualization, investigation. All authors have read and agreed to the published version of the manuscript.

## Conflicts of Interest

The authors declare no conflict of interest.

## References


1. Karabiber A, Keles C, Kaygusuz A, Alagoz BB. An approach for the integration of renewable distributed generation in hybrid DC/AC microgrids. Renew Energy. 2013;52. doi:10.1016/j.renene.2012.10.041
2. Nallolla CA, Vijayapriya P, Chittathuru D, Padmanaban S. Multi-Objective Optimization Algorithms for a Hybrid AC/DC Microgrid Using RES: A Comprehensive Review. Electron. 2023;12(4). doi:10.3390/electronics12041062
3. Safitri N, Shiddiq Yunus AM, Fauzi F, Naziruddin N. Integrated arrangement of advanced power electronics through hybrid smart grid system. Telkomnika (Telecommunication Comput Electron Control. 2020;18(6). doi:10.12928/telkomnika.v18i6.13433
4. Rabiul Islam M, Mahfuz-Ur-Rahman AM, Muttaqi KM, Sutanto D. State-of-The-Art of the Medium-Voltage Power Converter Technologies for Grid Integration of Solar Photovoltaic Power Plants. IEEE Trans Energy Convers. 2019;34(1). doi:10.1109/TEC.2018.2878885
5. Shabani M, Dahlquist E, Wallin F, Yan J. Techno-economic impacts of battery performance models and control strategies on optimal design of a grid-connected PV system. Energy Convers Manag. 2021;245. doi:10.1016/j.enconman.2021.114617
6. Zhi Y, Yang X. Scenario-based multi-objective optimization strategy for rural PV-battery systems. Appl Energy. 2023;345. doi:10.1016/j.apenergy.2023.121314
7. Kerdphol T, Qudaih Y, Watanabe M, Mitani Y. RBF neural network-based online intelligent management of a battery energy storage system for stand-alone microgrids. Energy Sustain Soc. 2016;6(1). doi:10.1186/s13705-016-0071-2
8. Fujimoto Y, Murakami S, Kaneko N, Fuchikami H, Hattori T, Hayashi Y. Machine learning approach for graphical model-based analysis of energy-aware growth control in plant factories. IEEE Access. 2019;7. doi:10.1109/ACCESS.2019.2903830
9. M. Urbano E, Martínez Viol V. Energy Infrastructure of the Factory as a Virtual Power Plant: Smart Energy Management. In: New Trends in the Use of Artificial Intelligence for the Industry 4.0. ; 2020. doi:10.5772/intechopen.88861
10. Sangadji IBM, Indrianto, Affandi Siregar RR. Early Warning Monitoring Model for Age of Household Electrical Appliances Using Adaptive Linear Neural Network (Adaline). Proc ICMERALDA 2023 - Int Conf Model E-Information Res Artif Learn Digit Appl. Published online 2023:272-276. doi:10.1109/ICMERALDA60125.2023.10458181
11. Alshammari M, Duffy M. Review of Single-Phase Bidirectional Inverter Topologies for Renewable Energy Systems with DC Distribution. Energies. 2022;15(18). doi:10.3390/en15186836
12. Shafiee-Rad M, Sadabadi MS, Shafiee Q, Reza Jahed-Motlagh M. Modeling and robust structural control design for hybrid AC/DC microgrids with general topology. Int J Electr Power Energy Syst. 2022;139. doi:10.1016/j.ijepes.2022.108012
13. Thirugnanam K, El Moursi MS, Khadkikar V, Zeineldin HH, Hosani M Al. Energy Management Strategy of a Reconfigurable Grid-Tied Hybrid AC/DC Microgrid for Commercial Building Applications. IEEE Trans Smart Grid. 2022;13(3). doi:10.1109/TSG.2022.3141459
14. Peña-Alzola R, Bianchi MA, Ordonez M. Control Design of a PFC with Harmonic Mitigation Function for Small Hybrid AC/DC Buildings. IEEE Trans Power Electron. 2016;31(9). doi:10.1109/TPEL.2015.2499163
15. Heo J, Moon H, Chang S, Han S, Lee DE. Case study of solar photovoltaic power-plant site selection for infrastructure planning using a bim-gis-based approach. Appl Sci. 2021;11(18). doi:10.3390/app11188785

16. Craciunescu D, Fara L. Investigation of the Partial Shading Effect of Photovoltaic Panels and Optimization of Their Performance Based on High-Efficiency FLC Algorithm. Energies. 2023;16(3). doi:10.3390/en16031169
17. Xu Y, Li Y, Chen Y, Zhou W, Mai R, He Z. A Multiple-Gain-Reconfigurable-Rectifier-Based IPT System for Battery Multistage Constant-Current High-Efficiency Wireless Charging. IEEE Trans Power Electron. 2024;39(1). doi:10.1109/TPEL.2023.3325471
18. Khalid HM, Rafique Z, Muyeen SM, et al. Dust accumulation and aggregation on PV panels: An integrated survey on impacts, mathematical models, cleaning mechanisms, and possible sustainable solution. Sol Energy. 2023;251. doi:10.1016/j.solener.2023.01.010
19. Talwar P, Verma N, Khatri H, et al. A systematic review of photovoltaic-green roof systems in different climatic conditions focusing on sustainable cities and societies. Sustain Cities Soc. 2023;98. doi:10.1016/j.scs.2023.104813
20. Prince Winston D, Kumaravel S, Praveen Kumar B, Devakirubakaran S. Performance improvement of solar PV array topologies during various partial shading conditions. Sol Energy. 2020;196. doi:10.1016/j.solener.2019.12.007
21. Lo Franco F, Morandi A, Raboni P, Grandi G. Efficiency comparison of DC and AC coupling solutions for large-scale PV+BESS power plants. Energies. 2021;14(16). doi:10.3390/en14164823
22. Lopez-Bernal D, Balderas D, Ponce P, Molina A. Education 4.0: Teaching the basics of knn, lda and simple perceptron algorithms for binary classification problems. Futur Internet. 2021;13(8). doi:10.3390/fi13080193
23. Park M, Seo M, Song Y, Kim SW. Capacity Estimation of Li-Ion Batteries Using Constant Current Charging Voltage with Multilayer Perceptron. IEEE Access. 2020;8. doi:10.1109/ACCESS.2020.3028095